Experimental Hematology & Oncology

CORRESPONDENCE Open Access

Exploring whether ChatGPT-4 with image analysis capabilities can diagnose osteosarcoma from X-ray images

Yi Ren[1,2†], Yusheng Guo[1,2†], Qingliu He[3,4†], Zhixuan Cheng[1,2], Qiming Huang[5*] and Lian Yang[1,2*]

Abstract

The generation of radiological results from image data represents a pivotal aspect of medical image analysis. The latest iteration of ChatGPT-4, a large multimodal model that integrates both text and image inputs, including dermatoscopy images, histology images, and X-ray images, has attracted considerable attention in the field of radiology. To further investigate the performance of ChatGPT-4 in medical image recognition, we examined the ability of ChatGPT-4 to recognize credible osteosarcoma X-ray images. The results demonstrated that ChatGPT-4 can more accurately diagnose bone with or without significant space-occupying lesions but has a limited ability to differentiate between malignant lesions in bone compared to adjacent normal tissue. Thus far, the current capabilities of ChatGPT-4 are insufficient to make a reliable imaging diagnosis of osteosarcoma. Therefore, users should be aware of the limitations of this technology.

Keywords ChatGPT-4, X-ray image, Osteosarcoma, Diagnosis

To the editor,

The generation of radiological results from image data is essential for medical image analysis. The most recent version of ChatGPT-4(Generative Pre-Training Transformer), a large multimodal model capable of integrating text and image inputs such as dermatoscopic [1], pathology [2], and X-ray images simultaneously [3, 4], is of significant interest to the field of radiology. In order to assess the performance of ChatGPT-4 in medical imaging image recognition, we conducted a study to evaluate its ability to accurately identify osteosarcoma X-ray images from real-world datasets.

We conducted a random selection of 40 cases each of lower limb osteosarcoma and normal lower limb bone X-ray images from the Picture Archiving and Communication System (PACS), ensuring that the images displayed typical characteristics of the condition and were accompanied by a pathological diagnosis of osteosarcoma. Following this, we obtained magnified representative images of lower limb osteosarcomas alongside images of normal lower limb bones. Specifically, to suggest the relationship between ChatGPT-4 lesions and adjacent anatomical structures, each of the osteosarcoma images contained portions of normal bone (Fig. 1A). However, the lesion sites remained more prominent in the images,

†Yi Ren, Yusheng Guo and Qingliu He contributed equally to this work.

*Correspondence:
Qiming Huang
hqmdoctor@163.com
Lian Yang
yanglian@hust.edu.cn
[1] Department of Radiology, Union Hospital, Tongji Medical College, Huazhong University of Science and Technology, No.1277 Jiefang Avenue, Wuhan 430022, China
[2] Hubei Key Laboratory of Molecular Imaging, Wuhan 430022, China
[3] Department of Urology, The Second Affiliated Hospital of Fujian Medical University, Quanzhou 362000, China
[4] Department of Urology, Union Hospital, Tongji Medical College, Huazhong University of Science and Technology, Wuhan 430022, China
[5] Department of Invasive Technology, The Second Affiliated Hospital of Fujian Medical University, Quanzhou 362000, China

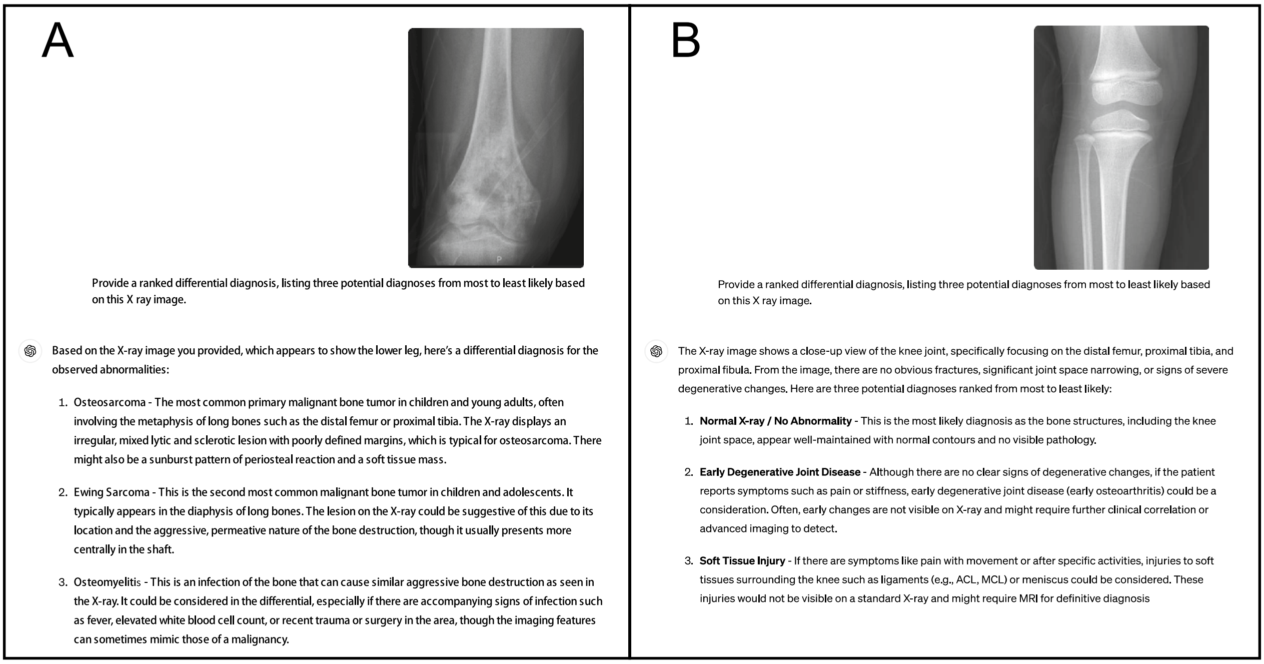

Provide a ranked differential diagnosis, listing three potential diagnoses from most to least likely based on this X ray image.

Based on the X-ray image you provided, which appears to show the lower leg, here's a differential diagnosis for the observed abnormalities:

1. Osteosarcoma - The most common primary malignant bone tumor in children and young adults, often involving the metaphysis of long bones such as the distal femur or proximal tibia. The X-ray displays an irregular, mixed lytic and sclerotic lesion with poorly defined margins, which is typical for osteosarcoma. There might also be a sunburst pattern of periosteal reaction and a soft tissue mass.
2. Ewing Sarcoma - This is the second most common malignant bone tumor in children and adolescents. It typically appears in the diaphysis of long bones. The lesion on the X-ray could be suggestive of this due to its location and the aggressive, permeative nature of the bone destruction, though it usually presents more centrally in the shaft.
3. Osteomyelitis - This is an infection of the bone that can cause similar aggressive bone destruction as seen in the X-ray. It could be considered in the differential, especially if there are accompanying signs of infection such as fever, elevated white blood cell count, or recent trauma or surgery in the area, though the imaging features can sometimes mimic those of a malignancy.

Provide a ranked differential diagnosis, listing three potential diagnoses from most to least likely based on this X ray image.

The X-ray image shows a close-up view of the knee joint, specifically focusing on the distal femur, proximal tibia, and proximal fibula. From the image, there are no obvious fractures, significant joint space narrowing, or signs of severe degenerative changes. Here are three potential diagnoses ranked from most to least likely:

1. **Normal X-ray / No Abnormality** - This is the most likely diagnosis as the bone structures, including the knee joint space, appear well-maintained with normal contours and no visible pathology.
2. **Early Degenerative Joint Disease** - Although there are no clear signs of degenerative changes, if the patient reports symptoms such as pain or stiffness, early degenerative joint disease (early osteoarthritis) could be a consideration. Often, early changes are not visible on X-ray and might require further clinical correlation or advanced imaging to detect.
3. **Soft Tissue Injury** - If there are symptoms like pain with movement or after specific activities, injuries to soft tissues surrounding the knee such as ligaments (e.g., ACL, MCL) or meniscus could be considered. These injuries would not be visible on a standard X-ray and might require MRI for definitive diagnosis

Fig. 1 Example of dialogue with ChatGPT-4 V providing a brief description of the X-ray image picture and a differential diagnosis of the bone X-ray image picture. **A** Lower limb osteosarcoma. **B** Normal lower limb bone

as evidenced by the results of ChatGTP-4 identification of the presence or absence of occupying lesions (Table 1). In order to align with the osteosarcoma images, the normal lower limb bone images were also partially enlarged to include joints and half of the long bones (Fig. 1B). All chosen images underwent validation by a senior radiologist (L.Y.) before being inputted into ChatGPT-4 ('December 2023 version') on the dates of May 11th to May 12th, 2024. The model was tasked with generating a ranked differential diagnosis, presenting three potential diagnoses in order of likelihood (Fig. 1). To avoid affecting the performance of ChatGPT-4, we did not give it any prior prompts, and normal bone images and osteosarcoma images were entered randomly into ChatGPT-4 [5]. X-ray images of osteosarcoma and normal bone were randomly inputted for the primary (Top-1) diagnosis and the priority diagnosis derived from the first three potential diagnoses. The target outcome, ranging from coarse to fine, includes identifying between occupying and non-occupying lesions, as well as between malignant and non-malignant lesions, osteosarcoma and non-osteosarcoma. Sensitivity, specificity, and overall diagnostic accuracy were calculated using the stats and epiR packages in R (version 4.2.1). The efficacy of ChatGPT-4 in detecting the presence or absence of occupying lesions, malignant lesions, and lesions indicative of osteosarcoma on bone X-ray images was evaluated.

Table 1 Sensitivity, specificity, and diagnostic accuracy of ChatGPT-4 in diagnosing osteosarcoma

Group	Sensitivity (95% CI)	Specificity (95% CI)	Accuracy (95% CI)
Occupied vs non-occupied			
Top 1	55.0% (39.8–69.3)	100.0% (91.2–100.0)	77.5% (67.2–85.3)
Priority	65.0% (49.5–77.9)	100.0% (91.2–100.0)	82.5% (72.7–89.3)
Malignant vs non-malignant			
Top 1	37.5% (24.2–53.0)	100.0% (91.2–100.0)	68.8% (57.9–77.8)
Priority	52.5% (37.5–67.1)	100.0% (91.2–100.0)	76.3% (65.9–84.2)
Correct diagnosis			
Top 1	20.0% (10.5–34.8)	100.0% (91.2–100.0)	60.0% (49.0–70.0)
Priority	35.0% (22.1–50.5)	100.0% (91.2–100.0)	67.5% (56.6–76.8)

According to the findings of the ChatGPT-4 analysis on osteosarcoma and normal bone production, various types of bone-occupying lesions were categorized into the occupied group, with primary and secondary malignant bone tumors, as well as bone tumors exhibiting malignant tendencies, being classified as malignant. Conversely, normal bone, deformities, and other non-occupying bone diseases were categorized into the non-occupying group. The results showed that ChatGPT-4 was effective in diagnosing bone with or without occupying lesions, achieving accuracies of 0.825 and 0.775 for priority and Top-1 diagnosis, respectively (Table 1). The sensitivities were 0.650 and 0.550, respectively, and the specificities were both 1; secondly, ChatGPT-4 exhibited higher accuracy in distinguishing between malignant and non-malignant bone conditions during priority diagnosis, achieving an accuracy of 0.763, a sensitivity of 0.525, and a specificity of 1. However, its performance in the Top-1 diagnosis was comparatively lower, with an accuracy of 0.688, a sensitivity of 0.375, and a specificity of 1. Moreover, ChatGPT-4 demonstrated limited proficiency in identifying osteosarcoma, as evidenced by priority diagnosis and Top-1 diagnosis accuracies of 0.675 and 0.600, respectively. The sensitivities for osteosarcoma detection were 0.350 and 0.200, while the specificities remained consistently high at 1. It is noteworthy that the sensitivity is low and the specificity is high in all the above results, suggesting that ChatGPT-4 is very accurate in detecting images without bone lesions. In addition, the most frequent misdiagnoses were giant cell tumour of bone (Top1: 5, top2: 1, top3: 1) and bone metastases (Top1: 5, top2: 1, top3: 2) (Supplementary Material).

Our assessment is constrained by several limitations, including a relatively small sample size, a lack of patient background information such as age and gender compared to typical clinical scenarios, and the absence of bilateral contrast images. Additionally, factors such as tumor size, shape, location, border definition, type of periosteal reaction, and pattern of bone destruction were not considered in the analysis. Our future research aims to increase the sample size and conduct replicated experiments to mitigate the impact of randomness, because ChatGPT-4 may provide varying responses to identical queries. Additionally, we intend to investigate the various factors that influence the diagnostic accuracy of ChatGPT-4 in detecting osteosarcoma. Despite being an exploratory study, our findings offer valuable insights into the potential application of ChatGPT-4 in medical imaging diagnosis. In conclusion, while ChatGPT-4 shows potential for enhancing various aspects of medical practice and can diagnose bone conditions with or without significant space-occupying lesions, these limitations should be taken into account when interpreting the results.

Abbreviation

PACS	Picture archiving and communication system

Supplementary Information

The online version contains supplementary material available at https://doi.org/10.1186/s40164-024-00537-z.

Supplementary Material 1.

Acknowledgements
The authors thank everyone who participated in this project and helped with this project.

Author contributions
Zhixuan Cheng conducted a comprehensive search and evaluation of relevant imaging images. Yi Ren, Yusheng Guo and Qingliu He provided the images to ChatGPT-4, which analyzed and interpreted the model diagnostic results. They were the main contributors to the writing of the manuscript. All authors read and approved the final manuscript.

Funding
None.

Data availability
Raw data already included in Supplementary Material 1.

Declarations

Ethics approval and consent to participate
The study's use of human imaging data was in full compliance with the World Medical Association's Declaration of Helsinki.

Consent for publication
Not applicable.

Competing interests
The authors declare no competing interests.

Received: 6 June 2024 Accepted: 9 July 2024
Published online: 27 July 2024

References

1. Shifai N, Van Doorn R, Malvehy J, Sangers TE. Can ChatGPT vision diagnose melanoma? An exploratory diagnostic accuracy study. J Am Acad Dermatol. 2024;90(5):1057–9.
2. Zhu L, Lai Y, Ta N, Cheng L, Chen R. Multimodal approach in the diagnosis of urologic malignancies: critical assessment of ChatGPT-4V's image-reading capabilities. JCO Clin Cancer Inform. 2024. https://doi.org/10.1200/CCI.23.00275.
3. Siepmann R, Huppertz M, Rastkhiz A, Reen M, Corban E, Schmidt C, et al. The virtual reference radiologist: comprehensive AI assistance for clinical image reading and interpretation. Eur Radiol. 2024. https://doi.org/10.1007/s00330-024-10727-2.
4. Zhou Y, Ong H, Kennedy P, Wu CC, Kazam J, Hentel K, et al. Evaluating GPT-V4 (GPT-4 with Vision) on detection of radiologic findings on chest radiographs. Radiology. 2024. https://doi.org/10.1148/radiol.233270.
5. Haotian Liu CL, Wu Q, Lee YJ. Visual instruction tuning.

Publisher's Note